


# LDH-A negatively regulates dMMR in colorectal cancer

Yongjie Zhang<sup>1</sup>  | Juan Li<sup>1</sup> | Bo Wang<sup>2</sup> | Ting Chen<sup>1</sup> | Yun Chen<sup>1</sup> | Wen Ma<sup>1</sup>

<sup>1</sup>Department of Medical Oncology, Huai'an Hospital Affiliated with Xuzhou Medical University, Huai'an, China

<sup>2</sup>Department of Anesthesiology, Huai'an Hospital of Traditional Chinese Medicine, Huai'an, China

## Correspondence

Yongjie Zhang, Department of Medical Oncology, Huai'an Hospital Affiliated with Xuzhou Medical University, Huai'an, Jiangsu Province 223002, China.  
Email: zhangyj0818@126.com

## Funding information

Huai'an Science and Technology Bureau, Grant/Award Number: HAB201818

## Abstract

Although immune checkpoint inhibitors (ICIs) have achieved unprecedented success in dMMR tumors, pMMR tumors accounting for 85% of colorectal cancer (CRC) cases remain unresponsive. Lactate dehydrogenase A (LDH-A) is the rate-limiting enzyme that catalyzes the transformation of pyruvate to lactate in the process of glycolysis. We investigated the relationship between LDH-A and dMMR with the purpose of exploring the treatment strategy for pMMR CRC patients. We here show that LDH-A can promote the proliferation of dMMR and pMMR CRC cells by positively regulating MMR proteins both in vitro and in vivo. LDH-A inhibition can improve the efficacy of PD-1 blockade in a pMMR CRC xenograft model. A statistical analysis of 186 CRC specimens showed a significant correlation between LDH-A and dMMR status. Moreover, patients with both low LDH-A expression and dMMR exhibited better disease-free survival compared with patients with other combinations. The close correlation of LDH-A and dMMR may offer a promising therapeutic strategy in which the combination of LDH-A inhibitor and ICIs may improve the clinical benefit for pMMR CRC patients.

## KEYWORDS

colorectal cancer, disease-free survival, lactate dehydrogenase A (LDH-A), mismatch-repair-deficient (dMMR), mismatch-repair-proficient (pMMR)

## 1 | INTRODUCTION

Colorectal cancer (CRC) is ranked in the top five cancer-related death causes despite dramatic advances in treatment.<sup>1</sup> Immune checkpoint inhibitors (ICIs), targeting co-inhibitory receptors, including cytotoxic T-lymphocyte-associated antigen 4 (CTLA-4) and programmed cell death protein 1 (PD-1) on T cells or ligands such as programmed cell death protein 1 ligand 1 (PD-L1) on tumor cells, have brought unprecedented clinical benefits in recent years and therefore are considered as milestones in oncology history. In CRC, it has been certificated that only patients with mismatch-repair-deficient or microsatellite-instability-high (dMMR/MSI-H) tumors

accounting for 15% of CRC cases are likely to respond to treatment with ICIs,<sup>2-4</sup> while mismatch-repair-proficient or microsatellite-instability-low (pMMR/MSI-L) tumors accounting for 85% of CRC cases are unresponsive. The dMMR/MSI-H subtype of CRC is characteristic of not only high tumor mutation burden (TMB)<sup>5</sup> derived from inactivation of 1 of the 4 mismatch-repair (MMR) genes: MSH2, MLH1, MSH6, PMS2,<sup>6-9</sup> but also of high immune cell infiltration, such as CD8<sup>+</sup> tumor-infiltrating lymphocytes (TIL) cell and T helper 1 (Th1) CD4<sup>+</sup> T cell promoting interferon gamma (IFN- $\gamma$ ) secretion. IFN- $\gamma$  plays an essential part in antitumor immunity and decreasing IFN- $\gamma$  production will inhibit the activity of CD8<sup>+</sup> T cells in the tumor microenvironment (TME).<sup>10</sup> The coexistence of harmful

Yongjie Zhang, Juan Li and Bo Wang contributed equally to this work.

This is an open access article under the terms of the Creative Commons Attribution-NonCommercial-NoDerivs License, which permits use and distribution in any medium, provided the original work is properly cited, the use is non-commercial and no modifications or adaptations are made.

© 2021 The Authors. *Cancer Science* published by John Wiley & Sons Australia, Ltd on behalf of Japanese Cancer Association.

TMB and favorable TME in perfect harmony suggests a potentially positive relationship between MMR genes and molecular pathways upregulating IFN- $\gamma$  in dMMR/MSI-H CRC.

Considering the important role in tumor development, the switch of immune state has attracted increasing attention. Both Th1 and Th2 are subtypes of helper T cells. Th1 cells secrete interleukin-2 (IL-2) and IFN- $\gamma$ , mediating CD8<sup>+</sup> T cells antitumor effects. Evaluation of the presence of tumor-infiltrating CD8<sup>+</sup> lymphocytes by immunoscore performs better compared with MSI/MMR status in predicting the prognosis of patients with early-stage CRC.<sup>11,12</sup> In contrast, Th2 cells promote tumor growth by inhibiting the production of Th1.<sup>13,14</sup> Th1 and Th2 cells maintain the homeostasis of immune system by cross-inhibiting each other. Impaired immunity is presented as switch from Th1 to Th2 and IFN- $\gamma$  downregulation. Therefore, promoting Th1 dominance is indispensable for successful treatment to reduce the risk of cancer progression. Cancer cells predominantly produce energy by a high rate of glycolysis followed by lactate fermentation, which is the famous Warburg effect. As an important rate-limiting enzyme, lactate dehydrogenase A (LDH-A) is responsible for transforming pyruvate into lactate in the process of glycolysis. The dependence of activated Th1 cells on glycolysis to gain energy calls for efficient export of lactate, leading to a gradient from cytoplasmic to extracellular lactate concentrations. However, intracellular accumulation of lactate resulting from the Warburg effect disturbs Th1 cell energy metabolism. Furthermore, lactate concentration can further decrease IFN- $\gamma$  by downregulating nuclear factor of activated T cells (NFAT) in Th1 cells. Therefore, increased lactate in cancer cells impairs IFN- $\gamma$  production, leading to inactivation of CD8<sup>+</sup> T cells and tumor development.<sup>15</sup> In contrast, LDH-A deficient tumors present as increased infiltration of CD8<sup>+</sup> T cells, resulting in elevation of IFN- $\gamma$  production. Compared with pMMR/MIS-L tumors, dMMR/MIS-H tumors are characterized by Th1 dominance with high IFN- $\gamma$  production. The negative correlation between LDH-A expression and IFN- $\gamma$  production suggests that LDH-A expression is relatively low in dMMR/MIS-H tumors. Further study indicated that dMMR tumors were associated with less vascular endothelial growth factor (VEGF) expression compared with pMMR/MSS tumors,<sup>16,17</sup> while LDH-A positively regulated VEGF in tumors.<sup>18</sup> It is therefore tempting to speculate that LDH-A in CRCs could be positively correlated with MMR proteins and relatively high LDH-A expression in pMMR CRCs may partly account for unresponsiveness to ICIs. As far as we know, this study is the first to investigate effects of LDH-A expression on MMR proteins.

In this study, we first detected LDH-A expression in CRC specimens, then investigated the association of its expression with clinical pathological parameters, dMMR, VEGF expression and disease-free survival (DFS). Furthermore, the effect of LDH-A on cell proliferation and the association of LDH-A expression with MMR proteins were studied in dMMR and pMMR CRC by *in vitro* and *in vivo* experiments. Our data demonstrated that LDH-A positively regulates MMR proteins in both dMMR and pMMR CRC and LDH-A inhibition can improve the efficacy of ICI in a pMMR CRC xenograft model. DFS of patients with both high LDH-A expression and pMMR is the

poorest. Therefore, LDH-A inhibitor combined with ICIs may provide clinical benefit for pMMR CRC patients.

## 2 | MATERIALS AND METHODS

### 2.1 | Cell lines

The dMMR cell line HCT116 and pMMR cell line SW480, purchased from the ATCC, were cultured in RPMI 1640 medium with 10% FBS.

### 2.2 | Construction of lentiviral vector and cell infection

Three shRNAs targeting LDH-A messenger RNA and blank-loaded transfection used as a negative control (NC) were designed and synthesized by the Biotechnology Company (GeneChem, Shanghai, China). The shRNA sequences are listed in Table S1. Three PLVX-Puro vectors with luciferase using lentiviral expression system, which contain LDH-A (LeLDH-A), shLDH-A (LeshLDH-A), or NC (LeNC), respectively, were designed and synthesized by the Biotechnology Company (GeneChem, Shanghai, China). The viral particles were packaged, amplified, titered in 293 cells and then applied to infect the dMMR cell line HCT116 and pMMR cell line SW480 in accordance with the manufacturer's specifications.

### 2.3 | Quantitative reverse transcription polymerase chain reaction

We extracted total RNA from the cells using ISOGEN (Nippon Gene). The cDNA was synthesized based on the protocol of the PrimeScript RT reagent Kit (TaKaRa, Kyoto, Japan). We performed real-time quantitative PCR reaction using KAPA SYBR FAST qPCR Kit (KAPA Biosystems). The primers for transcripts are listed in Table S2.

### 2.4 | Western blot

Extracted proteins were subjected to SDS-PAGE, blotted on PVDF membranes, and immunoblotted with antibodies for LDH-A, MLH1, MSH2, PMS2, MSH6, Oct4, and Sox2 (Abcam, AB Biotech Company Ltd., Cambridge, MA).

### 2.5 | Extracellular acidification and oxygen consumption rate assays

The extracellular acidification rate (ECAR) and cellular oxygen consumption rate (OCR) were examined using the Seahorse XF Glycolysis Stress Test Kit and Seahorse XF Cell Mito Stress Test Kit,

respectively. Seahorse XF-96 Wave software was used to assess data. OCR is shown in pmol/min and ECAR in mpH/min.

## 2.6 | Cell proliferation assay

Cells were seeded into 96-well plates at a density of 2000 cells/well. After incubation at 37°C for 6 d, the samples were treated with 20  $\mu$ L MTT reagent solution and cultured for 4 h. Then, we detected absorbance at 490 nm using an ELISA plate reader.

## 2.7 | dMMR CRC xenograft and lung metastasis model experiments

HCT116 cells transfected with LeLDH-A (overexpression, OE), LeshLDH-A (knockdown, KD), and LeNC (NC) were resuspended at  $5 \times 10^6$  cells/200  $\mu$ L in PBS and injected subcutaneously to establish a xenograft model or by caudal vein to make lung metastasis model. Here, 6-wk-old male BALB/c nude mice were purchased from the Second Military Medical University (Shanghai, China). Tumor size was determined by measuring 2 perpendicular diameters with a caliper at 3-d intervals. Tumor volume was calculated in accordance with the formula: volume ( $\text{mm}^3$ ) = width<sup>2</sup>  $\times$  length/2.

## 2.8 | pMMR CRC xenograft model experiments

SW480 cells transfected with LeshLDH-A (KD) or LeNC (NC) were resuspended at  $5 \times 10^6$  cells/200  $\mu$ L in PBS and injected subcutaneously to establish 4 xenograft models: NC, KD, NC + anti-PD-1 and KD + anti-PD-1. The mice in the anti-PD-1 treatment groups were intraperitoneally (ip) injected with 4 mg/kg body weight of anti-PD-1 mAb (Bioxcell, Lebanon, NH, USA) on days 10, 13, 16, 19, and 22.

## 2.9 | In vivo fluorescence imaging

At 1 h after 0.1 ml Cy7 signal peptide (1 mg/mL) was injected into BALB/c nude mice by tail vein, 10% chloral hydrate (3.5 mL per gram of body weight) was injected intraperitoneally to anesthetize the mice. Then, in vivo small animal imaging systems were applied to perform fluorescence scan-imaging of mouse tumors with an Ex/Em (nm) of 749/776. Tumor tissues were removed at the end of the experiment and subjected to histological study for the examination of MLH1, MSH2, PMS2, Oct4, and Ki67. We performed all procedures were in accordance with the Principles of Laboratory Animal Care. All animal studies were carried out based on the approved institutional animal care and use committee protocols at the Second Military Medical University.

## 2.10 | Patients, clinical specimens

In total, 186 patients (mean age, 59 y) with histologically confirmed primary CRC were enrolled in this study following curative surgery at Huai'an Hospital affiliated with Xuzhou Medical University from 2015 to 2019. None of the patients received neoadjuvant therapy. The 2-y clinical follow-up results were available for all patients. The median follow-up time was 7.9 mo (range: 3-22 mo). The use of all tissue specimens with patient informed consent was authorized by the Institutional Review Board of Huai'an Hospital affiliated with Xuzhou Medical University.

## 2.11 | Immunohistochemistry

All antibodies for LDH-A, VEGF, MLH1, MSH2, MSH6, PMS2, Oct4, and Ki67 were purchased from Abcam, AB Biotech Company Ltd., Cambridge, MA. Protein expression of MSH2, MLH1 and PMS2 in sections of mouse tumor samples was detected with the same antibodies as those used for the sections of CRC specimens. dMMR was defined as loss of immunohistochemistry expression of at least 1 of the MMR genes (MLH1, MSH2, MSH6, or PMS2). The cases that showed preserved nuclear expression of 4 MMR proteins were considered MMR proficient (pMMR). Grading scale of LDH-A was evaluated according to the scoring system as previously described.<sup>19</sup>

## 2.12 | Statistical analysis

Pearson's chi-squared ( $\chi^2$ ) test was used to evaluate the relationship between LDH-A and clinicopathological factors. Student *t* test was adopted when appropriate. We used the Mann-Whitney *U*-test to compare tumor volume. DFS of CRC patients was compared by Kaplan-Meier survival analysis and the difference of survival rates was evaluated by the log-rank test. We used the Cox proportional hazards model for multivariate survival analysis to assess the prognostic values. A *P*-value < .05 was considered to be statistically significant. All statistical analyses were performed using the SPSS statistical software program 16.0 for Microsoft Windows (SPSS Inc, Chicago, IL, USA).

## 3 | RESULTS

### 3.1 | Downregulation of LDH-A in dMMR CRC compared with pMMR CRC

Western blot was applied to detect LDH-A expression in dMMR cell line HCT116 and pMMR cell line SW480. SW480 exhibited significantly high levels of LDH-A expression compared with HCT116 cells (Figure 1A). Immunohistochemistry (IHC) results indicated that LDH-A expression was differentially downregulated in dMMR CRC specimens compared with pMMR CRC specimens, as was MSH2 and

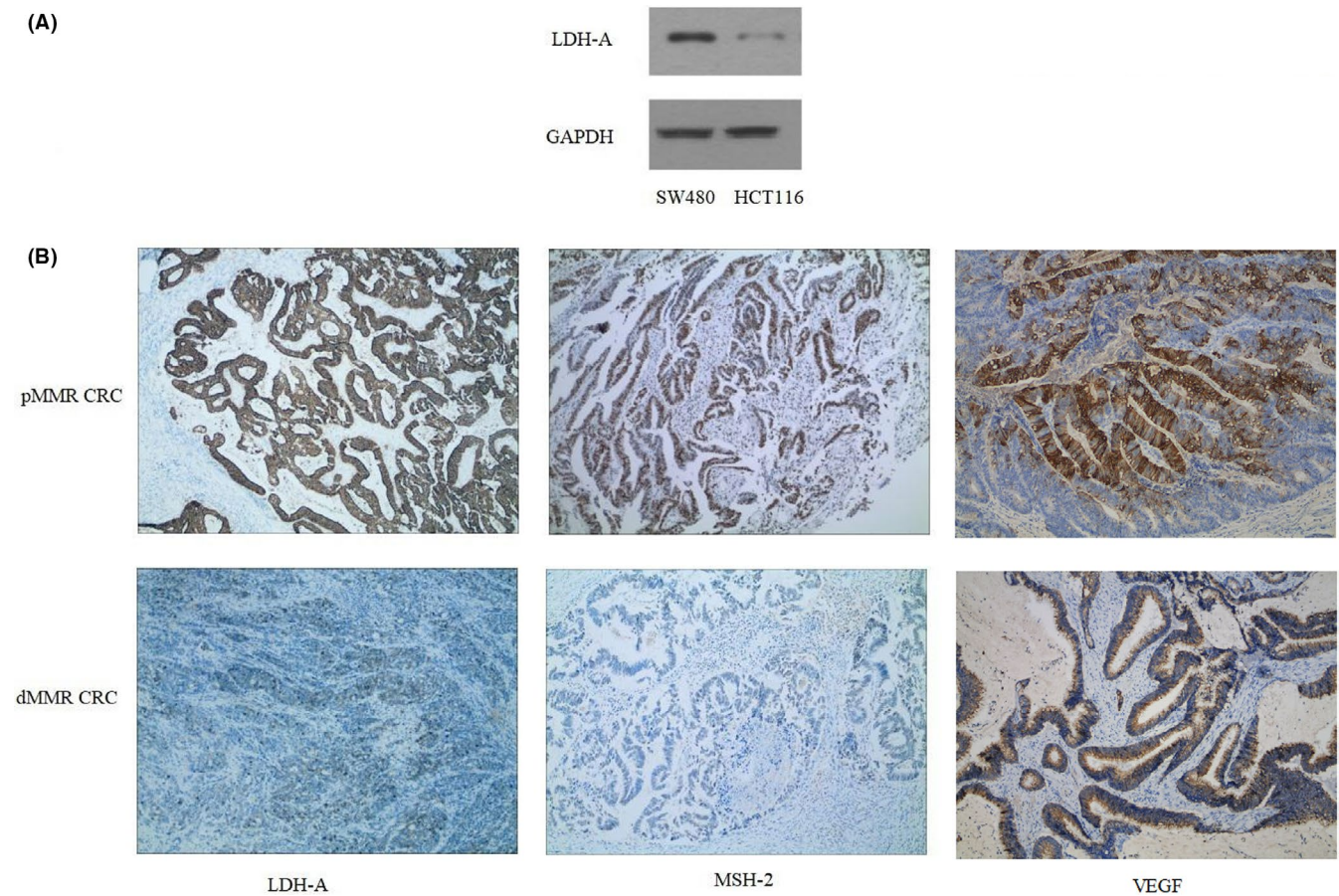


**FIGURE 1** Downregulation of LDH-A in dMMR CRC compared with pMMR CRC was confirmed by western blot and IHC. A, Expression of LDH-A in dMMR cell line HCT116 and pMMR cell line SW480 was determined by western blot. The LDH-A expression in the HCT116 cell line was downregulated compared with SW480. GAPDH was used as an internal control. B, IHC confirmed that both LDH-A and VEGF were downregulated in dMMR CRC tissues compared with pMMR CRC tissues

VEGF expression (Figure 1B). High LDH-A expression was detected in 9 of 29 (31.0%) dMMR CRC cases and in 82 of 157 (52.2%) pMMR CRC cases ( $P = .036$ ). The LDH-A expression was dramatically related to tumor location ( $P = .037$ ) and VEGF expression ( $P = .045$ ) (Pearson  $\chi^2$  test; Table 1). Altogether, our data indicated that LDH-A was downregulated in dMMR CRC.

### 3.2 | LDH-A positively regulates MMR proteins both in dMMR and pMMR cell lines

Based on the best inhibition of LDH-A expression at both mRNA and protein levels in dMMR cell line HCT116 cells (Figure 2A), shRNA667 was used for subsequent experiments. KD and OE dramatically decreased and increased LDH-A expression compared with NC, respectively, in accordance with the real-time RT-PCR and western blot results (Figure 2B). Significantly reduced extracellular acidification rate (ECAR) and enhanced cellular OCR were confirmed in the KD group, while opposite trends were found in the OE group (Figure S1). Our data indicated that LDH-A knockdown significantly inhibited HCT116 cells proliferation after the fourth

day following infection, and the number of viable cells sharply decreased with the suppression rate reaching 72% on the sixth day after infection. LDH-A overexpression significantly increased HCT116 cells proliferation after the third day following infection, and the number of viable cells sharply increased with the increase rate reaching 25% on the sixth day after infection (Figure 2C,D). To determine the relationship between LDH-A and dMMR, we detected the mRNA expression of MSH2, MSH6, MLH1, and PMS2 in the KD, OE, and control groups. Real-time PCR analysis revealed that the expression of MSH2, MLH1, and PMS2 was markedly reduced in the KD group ( $P < .001$ ), and markedly increased in the OE group ( $P < .001$ ), compared with the NC group. However, the expression of MSH6 remained unchanged (Figure 2E). The downregulation and upregulation of MSH2, MLH1, and PMS2 in the KD and OE groups, respectively, at the protein level were also confirmed by western blot (Figure 2F).

KD and OE dramatically decreased and increased LDH-A expression compared with NC in the pMMR cell line SW480 at both mRNA and protein levels (Figure 3A,B). Our data showed that proliferation capabilities were dramatically downregulated and upregulated in KD and OE groups, respectively, compared with NC group, as

**TABLE 1** Correlation between LDH-A and clinicopathological characteristics

| Clinicopathological factor | LDH-A expression |           | P-value |
|----------------------------|------------------|-----------|---------|
|                            | High (%)         | Low (%)   |         |
| Primary tumor location     |                  |           | .037    |
| Right                      | 56 (61.5)        | 44 (46.3) |         |
| Left                       | 35 (38.5)        | 51 (53.7) |         |
| Size                       |                  |           | .640    |
| ≥5 cm                      | 51 (56.0)        | 50 (52.6) |         |
| <5 cm                      | 40 (44.0)        | 45 (47.4) |         |
| Regional Lymph node        |                  |           | .153    |
| 0                          | 30 (33.0)        | 36 (37.9) |         |
| 1-3                        | 36 (39.6)        | 44 (46.3) |         |
| ≥4                         | 25 (27.5)        | 15 (15.8) |         |
| Differentiation            |                  |           | .296    |
| Well                       | 20 (22.0)        | 28 (29.5) |         |
| Moderately                 | 45 (49.5)        | 48 (50.5) |         |
| Poorly                     | 26 (28.6)        | 19 (20.0) |         |
| Primary TNM stage          |                  |           | .188    |
| I + II                     | 28 (30.8)        | 38 (40.0) |         |
| III                        | 63 (69.2)        | 57 (60.0) |         |
| Histologic subtype         |                  |           | .671    |
| Adenocarcinoma             | 68 (74.7)        | 66 (69.5) |         |
| Mucinous                   | 13 (14.3)        | 18 (18.9) |         |
| Mixed                      | 10 (11.0)        | 11 (11.6) |         |
| MMR status                 |                  |           | .036    |
| dMMR                       | 9 (9.9)          | 20 (21.1) |         |
| pMMR                       | 82 (90.1)        | 75 (78.9) |         |
| VEGF                       |                  |           | .045    |
| Positive                   | 61 (67.0)        | 50 (52.6) |         |
| Negative                   | 30 (33.0)        | 45 (47.4) |         |

confirmed by the number of viable cells in 3 groups on the sixth day after infection (Figure 3C,D). The downregulation and upregulation of MSH2, MLH1, and MSH6 in KD and OE groups, respectively, at both mRNA and protein levels were verified by RT-PCR and western blot (Figure 3E,F).

### 3.3 | The mechanism of LDH-A regulating MMR proteins

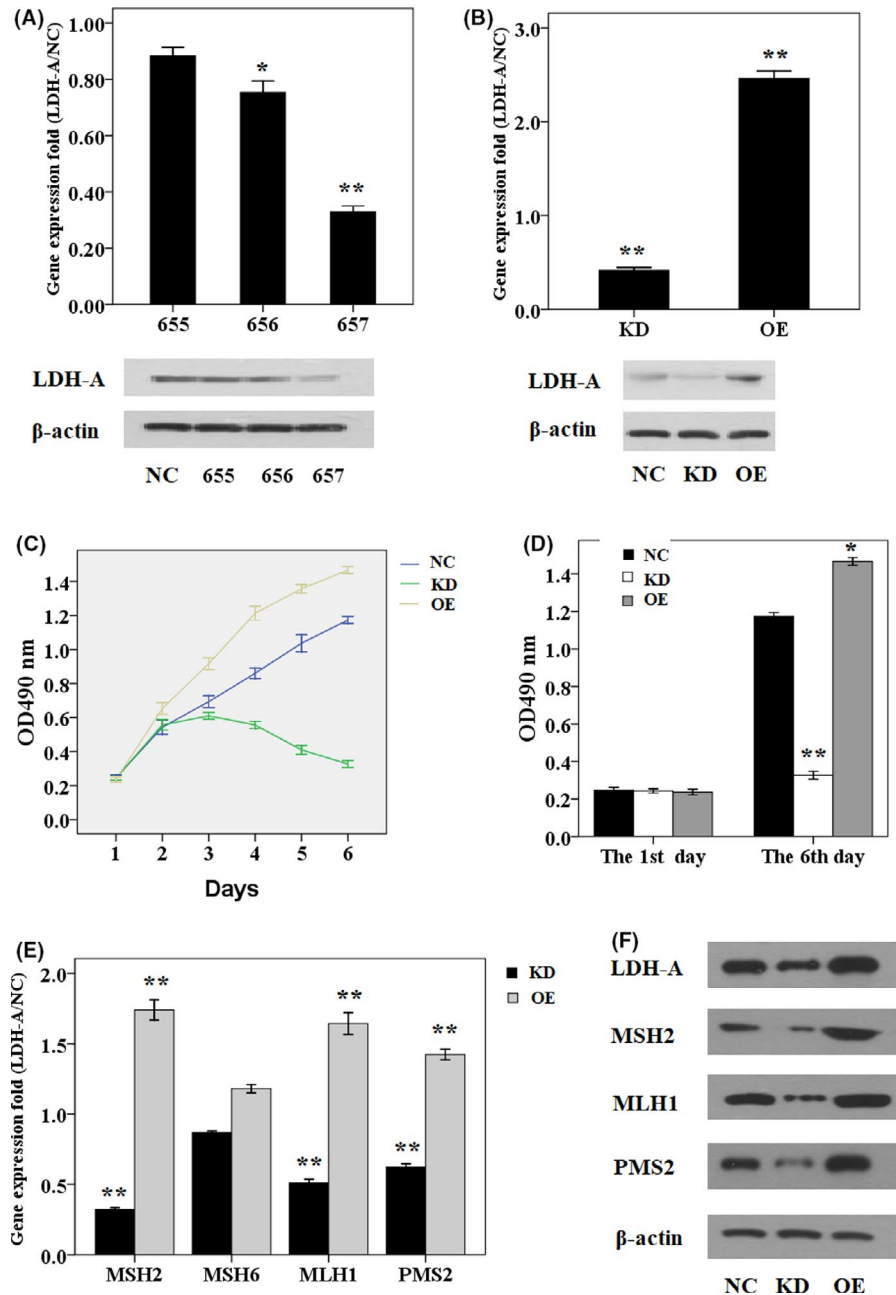
Increasing evidence has demonstrated the vital role of stemness genes in tumorigenesis and growth. Cells with high stemness such as cancer stem cells present an intrinsic property of inhibiting immunity by destructing cytotoxic T-cell responses.<sup>20</sup> Immune selection can also progressively convert a tumor into a stemness phenotype, which can dramatically suppress immunity,<sup>21</sup> highlighting the stemness characteristics of “cold tumor.” Induced pluripotent stem (iPS) cells can be successfully obtained by introducing

4 genes: Oct4, Sox2, Klf4, and c-Myc or Oct4, Sox2, NANOG, and LIN28 into differentiated cell types.<sup>22</sup> Oct4 and Sox2 constitute a core network of pluripotent gene regulation.<sup>23,24</sup> Indeed, Oct4 is the most principal gene for the induction of pluripotency and Sox2 is responsible for regulating Oct4.<sup>25</sup> Considering stemness plays a causative role in the formation of cold tumor microenvironments and LDH-A positively regulates stemness, we inferred LDH-A contributes to pMMR CRC by upregulating stemness genes. To confirm this postulation, we first compare stemness gene expression in dMMR and pMMR cell lines. Our data indicated that Oct4 and Sox2 were significantly decreased at mRNA and protein levels in dMMR cell line HCT16 compared with pMMR cell line SW480 (Figure 4A,B). LDH-A knockdown in SW480 cells significantly decreased mRNA and protein expression of Oct4 and Sox2 (Figure 4C,D). Altogether, LDH-A plays an important role in immunosuppressive TME of pMMR CRC by increasing stemness genes Oct4 and Sox2, implicating LDH-A as a shared therapeutic target to achieve the dual objectives of constraining tumor evolution and enhancing antitumor immunity.

### 3.4 | LDH-A positively regulates MMR proteins in dMMR CRC xenograft model

Based on our results, we inferred that LDH-A increased the proliferation capabilities of HCT116 cells by targeting dMMR and thereby destroying the adaptive immunity. To test whether LDH-A might promote CRC cell growth in vivo and if so, whether the mechanism is associated with the positive regulation of MSH2, MLH1 and PMS2, we made CRC cancer xenografts. The lack expression of MLH1 and PMS2 in HCT116 cells makes it difficult to compare IHC staining between KD and NC groups, although increased expression can be detected in the OE group compared with the NC group. Therefore, MSH2 IHC staining was used to explore further. Palpable nodules were identified 3 wk after the transplant of KD, while only 7 d after the transplant of NC, indicating that LDH-A knockdown impaired the capacity to initiate tumors, which was further verified by the markedly low tumor growth rate and final volume of the KD group compared with the NC group (Figure 5A-C). Both tumor growth rate and final volume were increased in the OE group compared with the NC group (Figure 5A-C). The number of MSH2-positive, Oct4-positive and Ki67-positive cells/100 cells was dramatically decreased in the KD group, and was significantly increased in OE group, compared with NC group (Figure 5D,E). Lung metastasis models were established by tail intravenous injection with LDH-A overexpression and knockdown cells. The final volume of pulmonary metastases was significantly decreased in the KD group and increased in the OE group compared with the NC group ( $P < .001$ ; Figure 6A,B). The number of MSH2-positive cells/100 cells was significantly decreased in KD group compared with the control group (Figure 6A,C). Altogether, our results demonstrated the negative relationship between LDH-A and dMMR both in vitro and in vivo.

**FIGURE 2** LDH-A positively regulates MSH2, MLH1, and PMS2 in the dMMR cell line HCT116. A, LDH-AsiRNA657 exhibited the best inhibition of LDH-A at both the mRNA and protein levels. B, Marked downregulation and upregulation of LDH-A in KD and OE groups, respectively, were confirmed at both the mRNA and protein levels compared with the NC group. C, HCT116 cells proliferation was markedly decreased and increased in KD and OE groups, respectively, compared with the NC group. D, The number of viable cells sharply decreased and increased in the KD and OE groups on the sixth day after infection. Significant downregulation and upregulation of MSH2, MLH1, and PMS2 were detected after LDH-A knockdown and overexpression, respectively, at both mRNA (E) and protein levels (F).  $\beta$ -Actin was used as the internal control. Each value represents the mean  $\pm$  SD for triplicate samples. \* $P < .01$ , \*\* $P < .001$  (Student *t* test)



### 3.5 | LDH-A knockdown augments the efficacy of PD-1 blockade in pMMR CRC xenograft model through downregulating MSH2 and Oct4

Tumor growth rate and final volume in a xenograft model of pMMR CRC were increased compared with that in a xenograft model of dMMR CRC (Figure S2). To investigate whether LDH-A inhibition can impair the growth of pMMR cells and whether the combination of LDH-A downregulation and anti-PD-1 therapy can achieve better inhibition of tumor progression compared with anti-PD-1 monotherapy in pMMR CRC, we divided the pMMR CRC xenograft into 4 groups: NC, anti-PD-1, KD and KD + anti-PD-1. Our data demonstrated that tumor growth rate and final volume were significantly decreased in KD group and KD + anti-PD-1, compared with the NC

group and anti-PD-1 group, respectively (Figure 7A,B). Therefore, blocking LDH-A reverses the immunosuppression in pMMR CRC and synergizes with anti-PD-1 for tumor abrogation by decreasing the expression of MSH2, stemness gene *Oct4* and *ki67* (Figure 7B).

### 3.6 | Combination of LDH-A and MMR protein expression better predicts the prognosis

Univariate analysis revealed that CRC patients with high LDH-A expression exhibited significantly worse DFS (Log-rank test; Figure 8A), as did CRC patients with pMMR (Log-rank test; Figure 8B). IHC analysis revealed that the high expression rate of LDH-A was 31.0% and 52.2% in dMMR and pMMR tumors, respectively. There exists

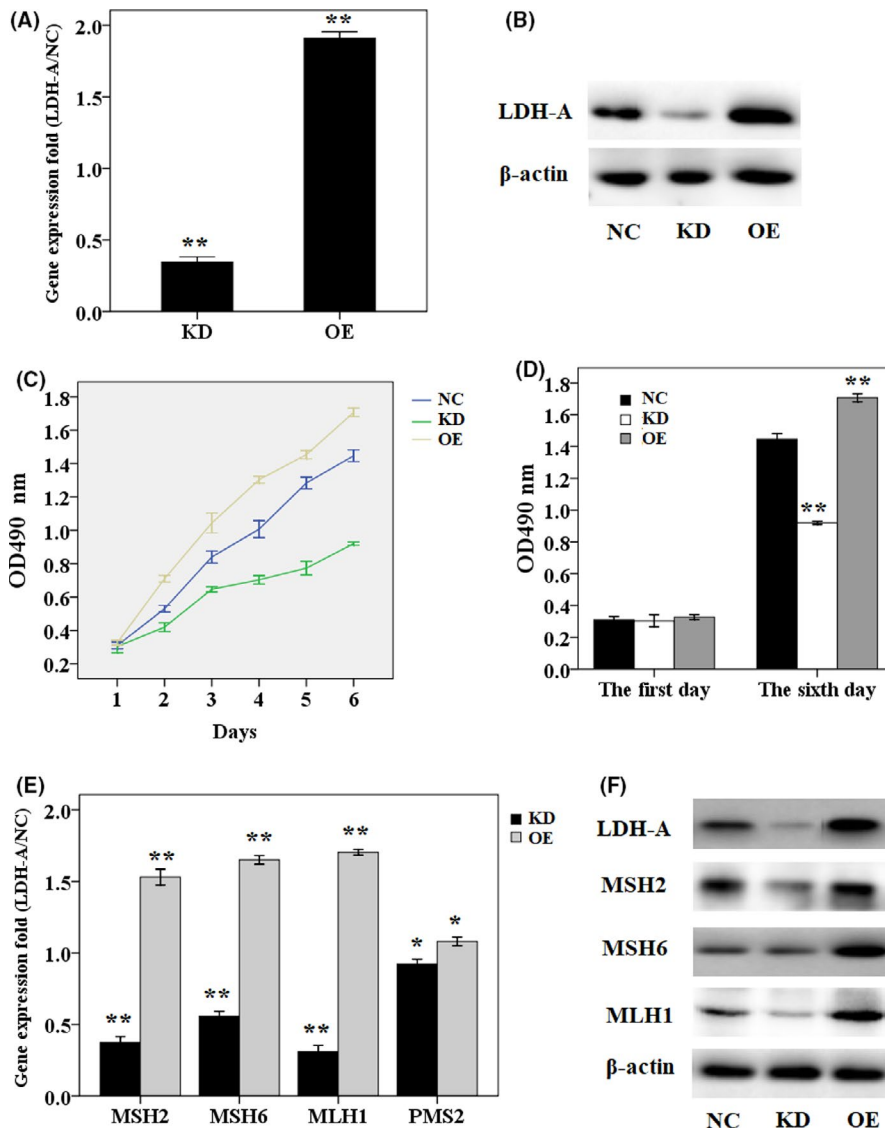


**FIGURE 3** LDH-A positively regulates MSH2, MLH1, and MSH6 in the pMMR cell line SW480. Marked downregulation and upregulation of LDH-A in the KD and OE groups, respectively, were confirmed at both the mRNA (A) and protein levels (B), compared with the NC group. C, SW480 cells proliferation was markedly decreased and increased in the KD and OE groups, respectively, compared with the NC group. D, The number of viable cells sharply decreased and increased in the KD and OE groups on the sixth day after infection. Significant downregulation and upregulation of MSH2, MLH1, and MSH6 were detected after LDH-A knockdown and overexpression, respectively, at both the mRNA (E) and protein levels (F).  $\beta$ -Actin was used as internal control. Each value represents the mean  $\pm$  SD for triplicate samples. \* $P < .01$ , \*\* $P < .001$  (Student *t* test)

significantly negative correlation between the high LDH-A expression and dMMR ( $P = .036$ , Table 1). With the purpose of investigating the potential relationship between the expression of LDH-A/MMR and the prognosis of CRC, we assessed the survival of patients in 4 groups: 1 subgroup with high LDH-A expression and pMMR, high LDH-A expression and dMMR, low LDH-A expression and pMMR, low LDH-A expression and dMMR. Univariate analysis showed that the DFS of patients with low LDH-A expression and dMMR were significantly better than that of other combinations in CRC ( $P < .001$ , Figure 5C). In a multivariate analysis, dMMR and LDH-A were independent prognostic factors for patients with stages I-III CRC after surgery (HR = 0.216; 95% CI: 0.053-0.637;  $P = .016$  and HR = 0.378; 95% CI: 0.063-0.695;  $P = .033$ , respectively).

## 4 | DISCUSSION

Following striking success in melanoma, ICI have already established a strong position in immunotherapy field of a wide

range of solid cancers including CRC. As an important marker of responsiveness to immunotherapy, mutation burden can induces neo-epitopes, which promote T-cell infiltration and therefore enhance immune activity,<sup>26,27</sup> which is counteracted by tumor cells by co-inhibitory receptors such as CTLA4, PD-1, and PD-L1. ICIs can receive suppressed immunity by targeting co-inhibitory receptors. Two ICIs: pembrolizumab and nivolumab were approved for treatment of dMMR-MSI-H mCRC by the FDA in 2017 in accordance with impressively favorable results from clinical trials. The success of PD1 inhibitors in dMMR-MSI-H CRC patients has attracted more attention on exploring underlying mechanism of this effect.

High mutational burden alone is insufficient for driving an immunotherapy response. Intricate tumor-immune interrelations endow tumor with metastatic potential. TME of dMMR CRC is characterized by increased CD8<sup>+</sup> T cells and PD-1/PD-L1 overexpression, indicative of a favorable prognosis. Furthermore, tumor-associated stroma also contributes to both good prognosis and dMMR status. Indeed, it has been verified that the improved outcome attributed to dMMR status is inextricably linked with such favorable TME. Elucidation of

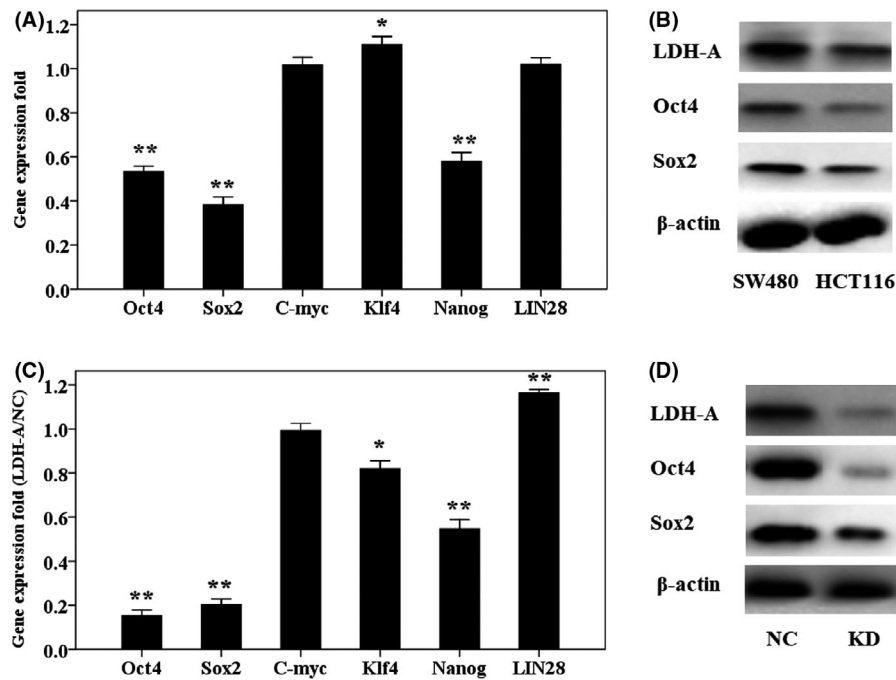


**FIGURE 4** Effect of LDH-A knockdown on the expression of stemness genes in the pMMR cell line SW480. A, The expression of Sox2, Oct4 and Nanog at the mRNA level was upregulated in the pMMR cell line SW480 compared with the dMMR cell line HCT116, while the mRNA expression of Klf4 was downregulated. B, Expression of Sox2 and Oct4 at the protein level was markedly upregulated in SW480 cells compared with HCT116 cells. C, Significant downregulation of Sox2, Oct4, Nanog, and Klf4 at mRNA level was detected after LDH-A knockdown in SW480 cells, while the mRNA expression of LIN28 was upregulated. D, Expression of Sox2 and Oct4 at the protein level was markedly downregulated after LDH-A knockdown in SW480 cells, as shown by western blot in the KD group compared with the NC group. The mRNA expression levels were normalized against β-actin. Each value represents the mean ± SD for triplicate samples. \* $P < .01$ , \*\* $P < .001$  (Student *t* test)

the underlying immunologic characteristics of TME will not only be useful for identifying patients who will benefit the most from ICIs, but also help to reveal the best target that could be taken advantage of to cooperate with ICIs. Therefore, exploring the relationship between MMR status and the microenvironment can undoubtedly provide a more efficient treatment strategy for CRC patients.

Cancer immune editing in TME can be described in 3 phases: elimination, equilibrium, and escape.<sup>28</sup> During the elimination phase, innate and adaptive immunity work in coordination with each other to eradicate tumor cells successfully. During the equilibrium phase, the continuous Darwinian selection process shields tumor cells from immune attack by upregulating checkpoint receptors such as CTLA-4, PD-1, PD-L1 and so on,<sup>29</sup> and downregulating antigen-presenting molecules. During the escape phase, continued deterioration of the immune environment breaks the stage of strategic stalemate between attacking immunity and defensive tumor eventually and promotes progression and metastasis.<sup>30,31</sup> Therefore, 3 phases of immunoediting indicate the dynamic decreasing process of immune response, presented as gradual decline trend of both body immunity and tumor immunogenicity. In dMMR tumors, dense immune infiltration demonstrates the stimulated immune system, which is counterbalanced by upregulation of multiple immune checkpoints that prevent tumor elimination, leading to immune tolerance and bringing an equilibrium phase into being. Large amounts of data have suggested that ICIs achieve the best effect in patients whose

endogenous immune response co-exists with the elevation of immune checkpoints.<sup>26,28-34</sup> Therefore, the upregulation of PD-L1 expression in the equilibrium phase plays an important role in adaptive immune escape by suppression of immune activity in TME. The clinical response to PD-1/PD-L1 blockade is restricted to patients whose inhibited immunity, at least in part, is attributable to PD-L1 expression.<sup>35,36</sup> Adaptive immune cell infiltration indicates favorable prognosis. The long-term survival of patients with dMMR/MSI-H-localized CRC is significantly associated with high immune infiltration. The phenomenon of seemingly paradoxical coexistence of tumor cells and tumor-specific CD8<sup>+</sup> T cells in dMMR tumors implies that dMMR genes and TME exist in harmony with each other, rather than in tension. Elucidation of an internal mechanism underlying the harmony could provide a new therapeutic target to further improve clinical effects of ICIs. Studies indicated that dMMR/MSI-H promotes immune infiltration and activation by IFN-γ secretion, which creates an "immune shield" and causes immune tolerance by upregulating PD-L1. Therefore, the signal pathway regulating IFN-γ plays a vital role in the close relationship between MMR/MSI-H and immunotherapy efficacy.

A prominent feature of tumor cells relative to normal cells is preferential utilization of glycolysis rather than mitochondrial oxidative phosphorylation despite the presence of oxygen, while energy metabolism of tumor-infiltrating T cells also depends on glycolysis. The increasing lactate accumulation in TME resulting



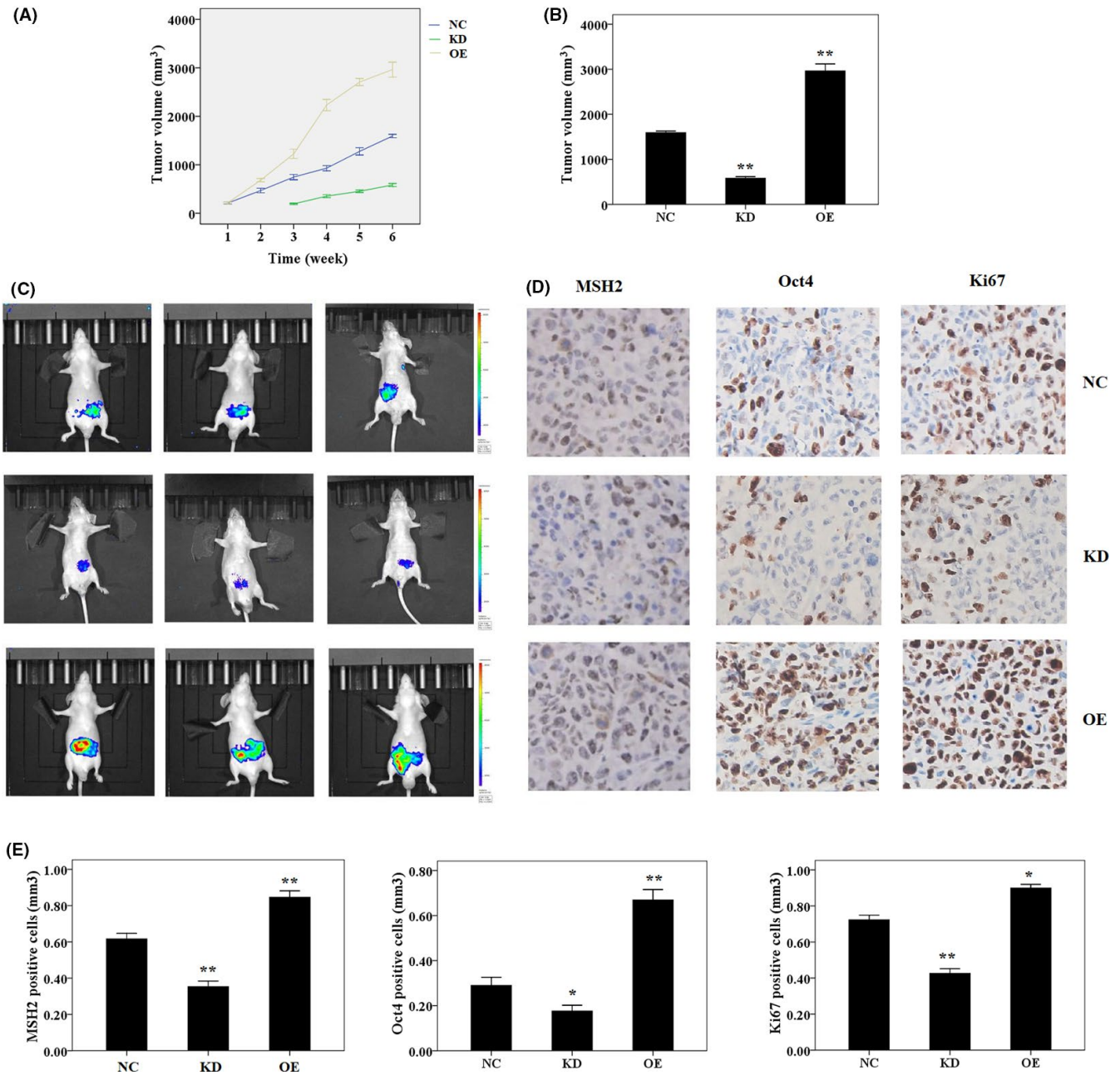


**FIGURE 5** LDH-A promotes tumorigenicity of dMMR cells. A, The significant difference in tumor growth rate in the KD and OE groups was observed, compared with the NC group at the corresponding time point. The significant difference in the final volume at week 6 in KD and OE groups was observed, compared with the NC group, as confirmed by quantification of expression (Mann-Whitney *U*-test) (B) and in vivo fluorescence imaging (C). D, The representative IHC image shows that MSH2-, Oct4-, and Ki67-positive cells were dramatically downregulated in the KD group, but upregulated in the OE group. E, Quantification of the expression of MSH2, Oct4, and Ki67 in both KD and OE groups. Each value represents the mean  $\pm$  SD. (Student *t* test). \**P* < .01, \*\**P* < .001

from tumor cells causes inactivation of T cells. Therefore, taking full advantage of the glycolytic characteristics of tumor cells and tumor-infiltrating T cells can achieve the dual effect of both killing tumors and enhancing immunity by decreasing lactate production. Glycolysis and the mitochondrial tricarboxylic acid cycle share the same pathway prior to pyruvate. LDH-A is an important rate-limiting enzyme transforming pyruvate into lactate in the process of glycolysis. Compared with inhibition of key glycolytic enzyme in metabolic processes prior to pyruvates such as hexokinase,

glucose-6-phosphate dehydrogenase (G6PD) and glyceraldehyde-3-phosphate dehydrogenase (GAPDH), targeting LDH-A can avoid damage to normal cell metabolism. Increased lactate in TME arising from LDH-A inhibits tumor immunosurveillance by downregulation of IFN- $\gamma$ .<sup>37</sup> Therefore, we infer that the favorable immune environment of dMMR relative to pMMR tumors is attributed to, at least in part, decreased LDH-A expression. Our data indicated that low LDH-A expression is positively correlated with dMMR in clinical specimens. The dMMR cell line HCT116 exhibited significantly

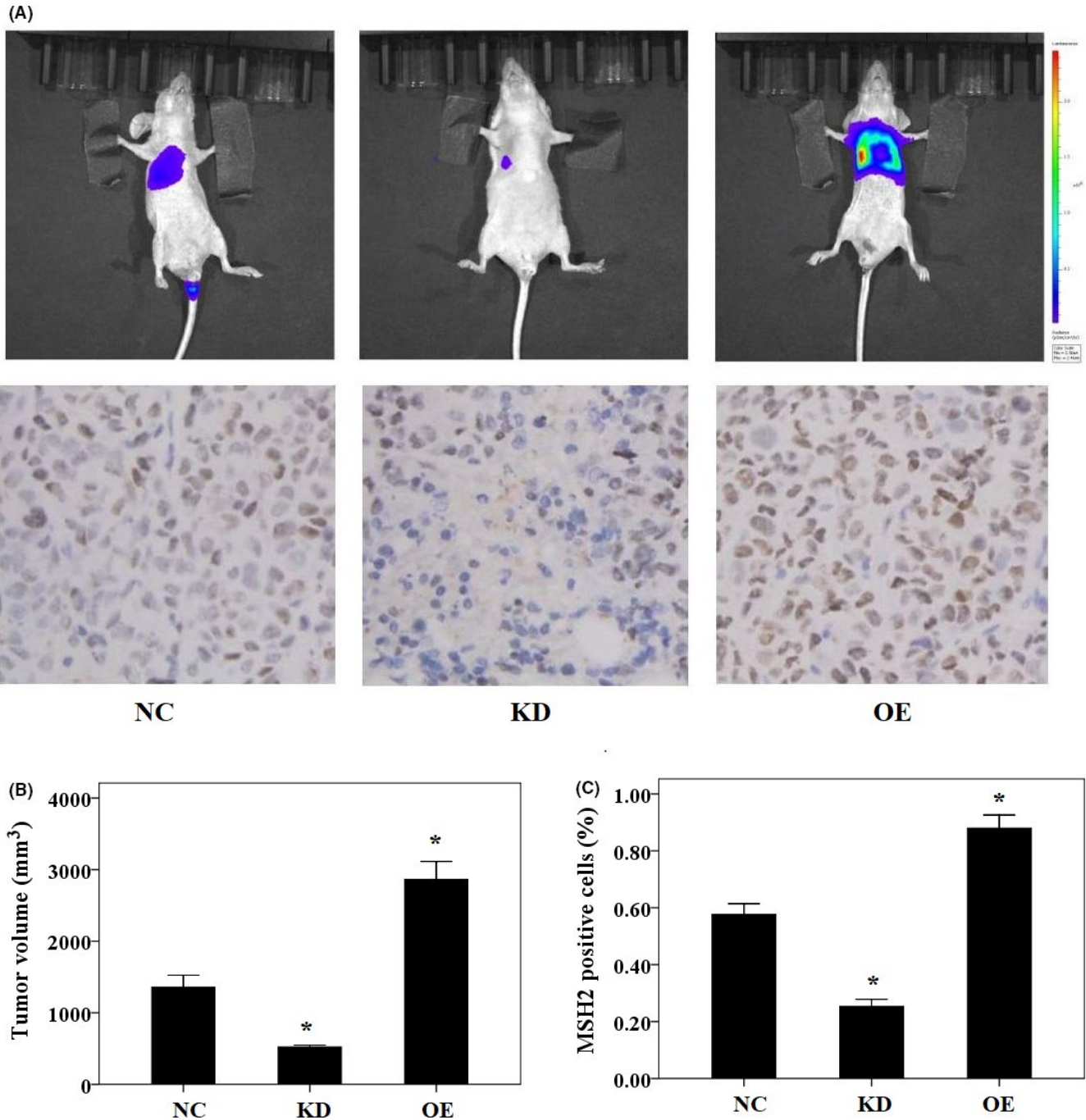


**FIGURE 6** LDH-A promotes lung metastasis of dMMR cells. A, In vivo fluorescence imaging in a mouse model of pulmonary metastatic tumor at week 6 indicated that fluorescence intensity of tumors in KD and OE groups was significantly decreased and increased, respectively, compared with that in the NC group (upper). IHC assay was used to detect MSH2 expression in both KD and OE groups. The representative image shows that MSH2-positive cells were significantly decreased and increased in the KD and OE groups, respectively (lower). B, Tumors in the KD and OE groups were significantly smaller and larger, respectively, than those in the control group in accordance with the final volume measurement (Mann-Whitney *U*-test). C, Quantification of MSH2 expression in both LDH-A knockdown and overexpression tumor samples. Each value represents the mean  $\pm$  SD. (Student *t* test). \**P* < .001

low levels of LDH-A expression compared with the pMMR cell line SW480. In vitro experiments confirmed that overexpression of LDH-A upregulates dMMR genes *MSH2*, *MLH1*, and *PMS2* at both mRNA and protein levels, while LDH-A knockdown downregulates *MSH2*, *MLH1*, and *PMS2* at both mRNA and protein levels. In vivo

experiments confirmed that MSH2-positive expression was significantly decreased in the LDH-A knockdown group, but dramatically increased in the LDH-A overexpression group, compared with the control group, in both CRC cancer xenografts and lung metastasis model of dMMR CRC.

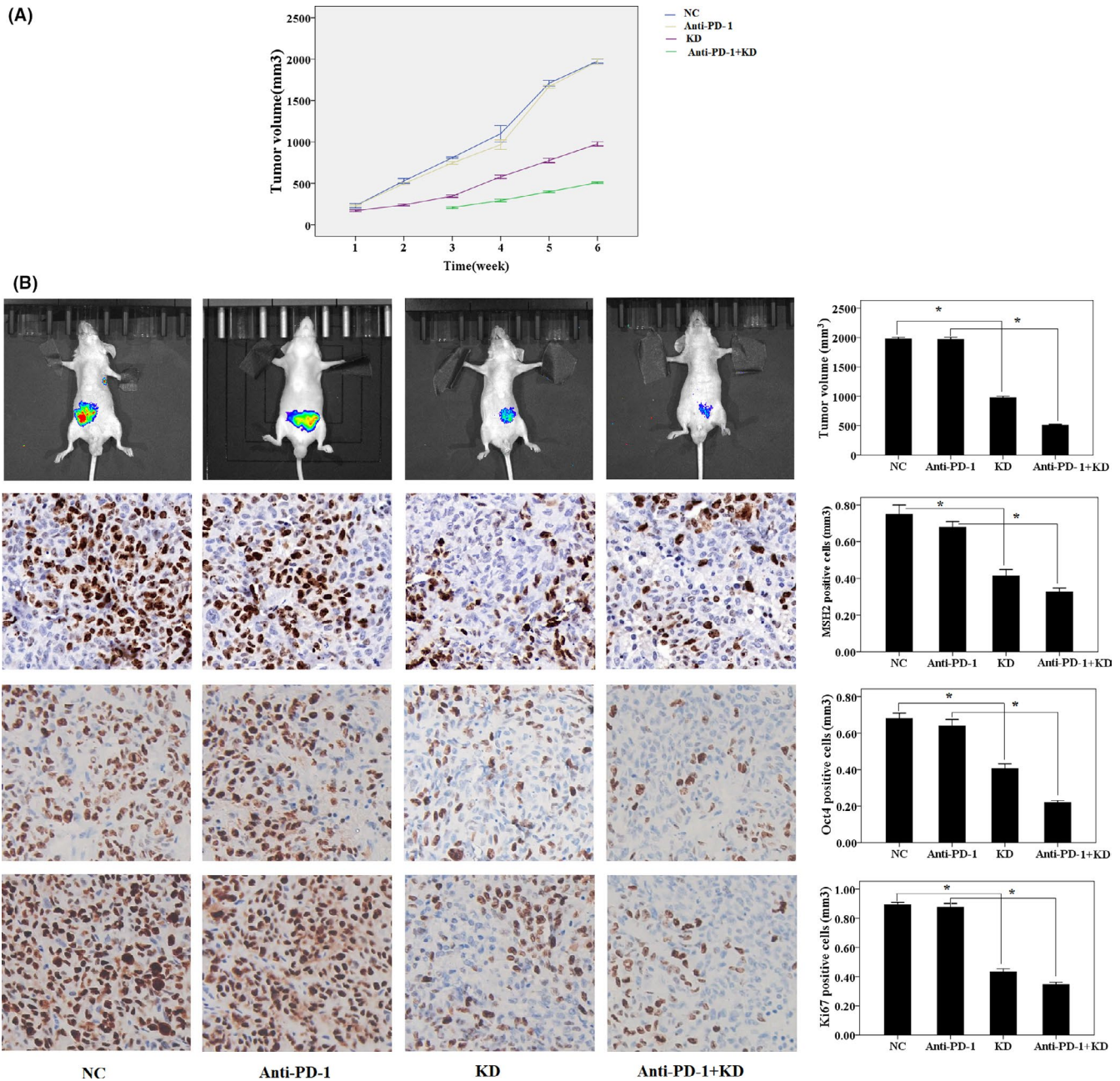
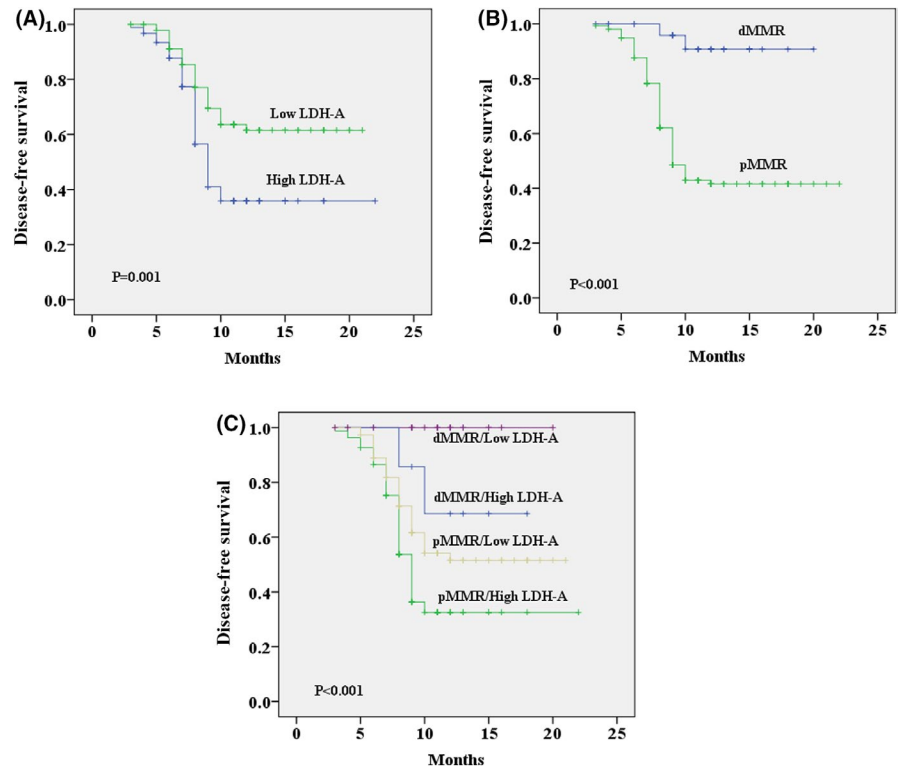


**FIGURE 7** LDH-A knockdown augments the efficacy of PD-1 blockade in pMMR CRC. Tumor growth rates were significantly decreased in the KD group and KD + anti-PD-1 group, compared with the NC group and anti-PD-1 group, respectively (A). The final volume as confirmed by quantification of expression (Mann-Whitney *U*-test) and in vivo fluorescence imaging (B). MSH2-, Oct4-, and Ki67-positive cells were dramatically downregulated in KD group and KD + anti-PD-1 group, compared with the NC group and anti-PD-1 group, respectively, as shown by the representative image and quantification of expression (B). Each value represents the mean  $\pm$  SD. (Student *t* test). \* $P < .001$

TME creates what is termed as “cold tumors,” leading to ineffective T-cell activation. Given the low response rate of ICI monotherapy, the spotlight has been on combining immunotherapy with multiple treatment modalities including chemotherapy, radiation, molecular targeted therapy or other immunotherapies with the purpose of transforming “cold tumors” into “hot tumors.” This transformation promotes antigen presentation, and enhances T-cell activation and penetration. The VEGF/vascular endothelial growth factor receptor (VEGFR) signal pathway is responsible for tumor

angiogenesis and immunosuppressive TME by upregulating PD-1/PD-L1. This marked efficiency was achieved from combining PD-1/PD-L1 blockade with VEGF/VEGFR inhibitors such as bevacizumab in a variety of tumors. A phase II study comparing clinical efficacy of PD-1 inhibitor in dMMR and pMMR CRC patients demonstrated that the objective response rate (ORR) was 0 for CRC patients with pMMR tumors vs 40% for those with dMMR tumors, suggesting that dMMR CRC belongs to “hot tumors” and pMMR CRC belongs to “cold tumors.” However, ORR was dramatically raised to be 36% for

**FIGURE 8** Prognosis analysis. A, The effect of LDH-A expression on DFS of CRC patients. B, The impact of MMR status on DFS of CRC patients. C, The DFS curves stratified in accordance with the combination of LDH-A expression and MMR status. DFS rates were estimated using Kaplan-Meier analyses. *P*-values (2-sided) were calculated using the log-rank test



pMMR CRC patients treated with PD-1 inhibitor plus regorafenib, a potent inhibitor for VEGFR tyrosine kinases.<sup>38</sup> Low VEGF expression and high treatment response to first-line 5-fluorouracil/leucovorin chemotherapy were verified in dMMR CRC compared with pMMR CRC.<sup>17</sup> These results indicated VEGF/VEGFR inhibitors can enhance the efficacy of ICIs by converting “cold tumors” into “hot tumors.” LDH-A is 1 of the upstream regulators of VEGF. Our data indicated that LDH-A downregulation contributes to dMMR CRC and there exists a positive relationship between LDH-A and VEGF expression in CRC patients. Immune cell exclusion is widely associated with the presence of a stem cell-like phenotype in tumors. Stemness positively correlates with higher intratumoral heterogeneity, exhibiting an enhanced capacity for self-renewal, multipotency, and tumorigenicity and therefore playing an important role in the resistance, metastasis, and recurrence of tumors. The activation of a stemness program can inhibit effector T cells and limit antitumor immune responses by upregulation of VEGF and PD-1/PD-L1. Conversely, infiltrating immune cells interact with stemness genes to promote tumor progression. Previous studies demonstrated reciprocal interactions between LDH-A and stemness genes including core network *Sox2/Oct4* genes in deriving iPS cells. Our data indicated that LDH-A positively regulated MMR proteins both in dMMR and pMMR cell lines. Overall, LDH-A, stemness, VEGF, and impaired immunity constitute a positive cycle, accounting for tumor progression in a cooperative manner. Therefore, we deduced that high LDH-A expression contributed to the “cold” characteristics of pMMR CRC and that LDH-A inhibition can improve efficacy of anti-PD-1 treatment by transforming “cold tumors” into “hot tumor” by downregulating stemness genes expression. Our work demonstrated that the expression of LDH-A, Oct4, and Sox2 at both the mRNA and protein

levels was significantly upregulated in the pMMR cell line SW480, compared with the dMMR cell line HCT116. Further study indicated that LDH-A downregulation in SW480 cells markedly decreased the expression of Oct4 and Sox2, as shown by RT-PCR and western blot. In vivo pMMR CRC xenograft experiments demonstrated that LDH-A inhibition significantly decreased tumor growth rate and final volume, as well as MSH2-, Oct4-, and Ki67-positive cells, consistent with the results of the in vitro experiment. Tumor growth rate and final volume were also markedly reduced by LDH-A inhibition combined with anti-PD-1 treatment compared with anti-PD-1 monotherapy, as were MSH2-, Oct4-, and Ki67-positive cells. Therefore, reversing the stemness phenotype by LDH-A inhibition in pMMR CRC would render tumors more responsive to ICIs. We concluded that the relatively high LDH-A expression in pMMR CRC compared with dMMR CRC contributed to immunosuppression by upregulating Oct4. Also LDH-A positively regulated MSH2, Oct4, and ki67 in a dMMR CRC xenograft model. In other words, high LDH-A expression was responsible for “cold tumors,” possibly due to 3 factors. First, LDH-A constitutes a bottleneck suppression of T-cell activation by increasing lactate concentration in TME. Second, LDH-A inhibits tumor-infiltrating T cells and NK cells from producing IFN- $\gamma$ , which mediates immune infiltration and activation in dMMR/MSI-H tumors. Third, LDH-A promotes an immunosuppressive microenvironment by upregulating stemness genes and VEGF. Altogether, low LDH-A expression can contribute to bringing “hot tumors” into being, and is an essential prerequisite for favorable clinical outcome and impressive benefits from ICIs in dMMR tumors.

Univariate analysis indicated that both dMMR and low LDH-A expression can predict good prognosis in CRC. Given that a negative relationship was found between LDH-A expression and dMMR,

we investigated whether the combination of LDH-A expression and MMR status could predict the outcome more efficiently. As expected, the CRC patients with both high LDH-A expression and pMMR had the poorest DFS. Therefore, the predictive value of LDH-A expression in combination with MMR status outperformed that of LDH-A or MMR alone. In mouse model of pulmonary metastatic tumor, both tumor size and MSH2-positive cells were significantly decreased in LDH-A knockdown group, while significantly increased in LDH-A overexpression group, demonstrating that LDH-A can promote progression by negatively regulating dMMR. Therefore, LDH-A may partner with MMR proteins synergistically both in CRC development and in tumorigenicity.

In conclusion, our study confirmed the close association of dMMR with low LDH-A expression in CRC by both in vitro and in vivo experiments. The negative impact of LDH-A on dMMR was further verified by an analysis of CRC tissue specimens and DFS. As far as we know, our data is the first to demonstrate the significantly intimate correlation between an energy metabolism-related enzyme and the expression of dMMR genes, which is 1 of the vital determinants of immunotherapy outcome.

Considering the limited efficacy of checkpoint inhibitors, combination of PD-1/PD-L1 monoclonal antibody with LDH-A inhibitor could provide a promising and efficient therapy for CRC patients, especially for pMMR CRC patients.

#### CONFLICT OF INTEREST

The authors declare no conflict of interest.

#### ORCID

Yongjie Zhang  <https://orcid.org/0000-0002-6731-4923>

#### REFERENCES

1. Ferlay J, Colombet M, Soerjomataram I, et al. Estimating the global cancer incidence and mortality in 2018: GLOBOCAN sources and methods. *Int J Cancer*. 2019;144:1941-1953.
2. Le DT, Uram JN, Wang H, et al. PD-1 blockade in tumors with mismatch-repair deficiency. *N Engl J Med*. 2015;372:2509-2520.
3. Overman MJ, McDermott R, Leach JL, et al. Nivolumab in patient with metastatic DNA mismatch repair-deficient or microsatellite instability-high colorectal cancer (CheckMate 142): an open-label, multicentre, phase 2 study. *Lancet Oncol*. 2017;18:1182-1191.
4. Overman MJ, McDermott R, Leach JL, et al. Durable clinical benefit with nivolumab plus ipilimumab in DNA mismatch repair-deficient/microsatellite instability-high metastatic colorectal cancer. *J Clin Oncol*. 2018;36:773-779.
5. Vogelstein B, Papadopoulos N, Velculescu VE, Zhou S, Diaz LA Jr, Kinzler KW. Cancer genome landscapes. *Science*. 2013;339:1546-1558.
6. Aaltonen LA, Peltomäki P, Leach FS, et al. Clues to the pathogenesis of familial colorectal cancer. *Science*. 1993;260:812-816.
7. Josef J. The multifaceted mismatch-repair system. *Nat Rev Mol Cell Biol*. 2006;7:335-346.
8. Strand M, Prolla TA, Liskay RM, Petes TD. Destabilization of tracts of simple repetitive DNA in yeast by mutations affecting DNA mismatch repair. *Nature*. 1993;365:274-276.
9. Ionov Y, Peinado MA, Malkhosyan S, Shibata D, Perucho M. Ubiquitous somatic mutations in simple repeated sequences reveal a new mechanism for colonic carcinogenesis. *Nature*. 1993;363:558-561.
10. Ganesh K, Stadler ZK, Cercek A, et al. Immunotherapy in colorectal cancer: rationale, challenges and potential. *Nat Rev Gastroenterol Hepatol*. 2019;16:361-375.
11. Bernhard M, Gabriela B, Helen KA, et al. Integrative analyses of colorectal cancer show immunoscore is a stronger predictor of patient survival than microsatellite instability. *Immunity*. 2016;44:698-711.
12. Franck P, Bernhard M, Florence M, et al. International validation of the consensus Immunoscore for the classification of colon cancer: a prognostic and accuracy study. *Lancet*. 2018;391(10135):2128-2139.
13. Patrick MD, Walter CO, Andrea C, et al. A melanoma helper peptide vaccine increases T1 cytokine production by leukocytes in peripheral blood and immunized lymph nodes. *J Immunother Cancer*. 2014;2:23.
14. Nagarsheth N, Kryczek I, Wei S, Frankel T, Zou WP. Regulatory T cells in tumor immunity. *Encyclopedia of Immunobiology*. 2016;4:451-459.
15. Kristen ENS, John LC. Lactate wreaks havoc on tumor-infiltrating T and NK cells. *Cell Metab*. 2016;24:649-650.
16. Zhang C, Lv JF, Gong L, et al. Role of deficient mismatch repair in the personalized management of colorectal cancer. *Int J Environ Res Public Health*. 2016;13:892.
17. Bendardaf R, Sharif-Askari FS, Sharif-Askari NS, Syrjänen K, Pyrhönen S. Patients with hMLH1 or/and hMSH2-deficient metastatic colorectal cancer are associated with reduced levels of vascular endothelial growth factor-1 expression and higher response rate to irinotecan-based regimen. *Anticancer Res*. 2018;38:6399-6404.
18. Inna S, Ivan JC, Kiranmayi V, et al. LDH-A regulates the tumor microenvironment via HIF-signaling and modulates the immune response. *PLoS One*. 2018;13:e0203965.
19. Jiang F, Ma S, Xue Y, Hou J, Zhang Y. LDH-A promotes malignant progression via activation of epithelial-to-mesenchymal transition and conferring stemness in muscle-invasive bladder cancer. *Biochem Biophys Res Commun*. 2016;469:985-992.
20. Bruttel VS, Wischhusen J. Cancer stem cell immunology: key to understanding tumorigenesis and tumor immune escape? *Front Immunol*. 2014;5:360.
21. Noh KH, Lee YH, Jeon JH, et al. Cancer vaccination drives Nanog-dependent evolution of tumor cells toward an immune-resistant and stem-like phenotype. *Cancer Res*. 2012;72:1717-1727.
22. Yu J, Vodyanik MA, Smuga-Otto K, et al. Induced pluripotent stem cell lines derived from human somatic cells. *Science*. 2007;318:1917-1920.
23. Rodda DJ, Chew JL, Lim LH, et al. Transcriptional regulation of nanog by OCT4 and SOX2. *J Biol Chem*. 2005;280:24731-24737.
24. Loh YH, Wu Q, Chew JL, et al. The Oct4 and Nanog transcription network regulates pluripotency in mouse embryonic stem cells. *Nat Genet*. 2006;38:431-440.
25. Kim JB, Zaehres H, Wu G, et al. Scholer. Pluripotent stem cells induced from adult neural stem cells by reprogramming with two factors. *Nature*. 2008;454:646-650.
26. Tumeh PC, Harview CL, Yearley JH, et al. PD-1 blockade induces responses by inhibiting adaptive immune resistance. *Nature*. 2014;515:568-571.
27. Michael SR, Sachet AS, Catherine JW, Gad G, Nir H. Molecular and genetic properties of tumors associated with local immune cytolytic activity. *Cell*. 2015;160:48-61.
28. Dunn GP, Old LJ, Schreiber RD. The three Es of cancer immunoeediting. *Annu Rev Immunol*. 2004;22:329-360.
29. Nicolas JL, Michael C, Ada T, et al. The vigorous immune microenvironment of microsatellite instable colon cancer is balanced by multiple counter-inhibitory checkpoints. *Cancer Discov*. 2015;5:43-51.
30. Ryungsa K, Manabu E, Kazuaki T. Cancer immunoeediting from immune surveillance to immune escape. *Immunology*. 2007;121:1-14.
31. Stewart TJ, Abrams SI. How tumours escape mass destruction. *Oncogene*. 2008;27:5894-5903.

32. Herbst RS, Soria JC, Kowanetz M, et al. Predictive correlates of response to the anti-PD-L1 antibody MPDL3280A in cancer patients. *Nature*. 2014;515:563-567.
33. Rizvi NA, Hellmann MD, Snyder A, et al. Cancer immunology. Mutational landscape determines sensitivity to PD-1 blockade in non-small cell lung cancer. *Science*. 2015;348:124-128.
34. Ji R-R, Scott DC, Wang L, et al. An immune-active tumor microenvironment favors clinical response to ipilimumab. *Cancer Immunol Immunother*. 2012;61:1019-1031.
35. Stefani S, Robbert MS, Zha YY, et al. Up-regulation of PD-L1, IDO T(regs) in the melanoma tumor microenvironment is driven by CD8(+) T cells. *Sci Transl Med*. 2013;5:200ra11.
36. Ji RR, Chasalow SD, Wang L, et al. An immune-active tumor microenvironment favors clinical response to ipilimumab. *Cancer Immunol Immunother*. 2012;61:1019-1031.
37. Almut B, Katrin S, Gudrun EK, et al. LDHA -associated lactic acid production blunts tumor immunosurveillance by T and NK cells. *Cell Metab*. 2016;24:657-671.
38. Fukuoka S, Hara H, Takahashi N, et al. Regorafenib plus Nivolumab in patients with advanced gastric or colorectal cancer: An open-label, dose-escalation, and dose-expansion phase Ib trial (REGONIVO, EPOC1603). *J Clin Oncol*. 2020;38:2053-2061.

#### SUPPORTING INFORMATION

Additional supporting information may be found online in the Supporting Information section.

**How to cite this article:** Zhang Y, Li J, Wang B, Chen T, Chen Y, Ma W. LDH-A negatively regulates dMMR in colorectal cancer. *Cancer Sci*. 2021;112:3050–3063. <https://doi.org/10.1111/cas.15020>